

Investigation of Soliton Propagation in Asymmetric metal-dielectric-metal Plasmonics Waveguide

M. Olyaei^{1*}, M.B. Tavakoli², A. Mokhtari³

^{1*}Department of OPTO Electronics, Azad University of Arak, Arak, Iran

²Department of OPTO Electronics, Azad University of Arak, Arak, Iran

³Department of OPTO Electronics, Azad University of Arak, Arak, Iran

Available online at: www.ijcseonline.org

Received: 12/Jan/2017

Revised: 23/Jan/2017

Accepted: 18/Feb/2017

Published: 31/Mar/2017

Abstract— In this paper, the propagation of soliton in metal-dielectric-metal (MDM) plasmonics waveguides was investigated for both nonasymmetric and asymmetric structures. Nonasymmetric effects such as Soliton are important for applications such as switching and wavelength conversion. In this paper, it was shown that field enhancement in nonasymmetric MDM waveguides can result in large enhancement of SOLITON magnitude compared to the literature values. Two different structures are considered here as plasmonics waveguide for generation of second harmonic. The first structure is a structure including of a Lithium Niobite as insulator sandwiched between two same metals. Thereafter, two different metals on both sides of the waveguide were used. Besides the structure has grating on both sides for more coupling between photons and plasmons. the wavelength The duration of grating per length unit (number of grooves) will be optimized to reach the highest second harmonic generation. To perform this optimization, the wavelength of operation of $\lambda=458$ nm is considered. It was shown that this asymmetric device results in more than two orders of magnitude enhancement in SOLITON compared to a structure with the same metals. It is also shown that the electric field of second harmonic depends on the thickness of crystal (insulator). So, its thickness is optimized to achieve the highest electric field.

Keywords— Plasmonics, Surface plasmons, Soliton

I. INTRODUCTION

In recent years, plasmonics devices have attracted considerable attention [1-4]. Generally, plasmonics can be considered as light on metal-dielectric interfaces. In this condition, electrons at the surface of metal are collectively accelerated and decelerated by the electric field of light with high frequency. This activity of electrons is similar to plasma. As electrons are involved in the propagation of light, it can be localized into sub-wavelength dimensions [5]. Particularly, a surface wave would be formed by oscillations of collective electrons that exponentially decay into two adjacent half spaces. This collective electronic surface wave that oscillates with the frequency of light is called surface plasmon (SP) mode. Although the field decays exponentially into two half spaces, it has an imaginary wave phase, which is propagated along the surface.

These accelerated electrons of metal may increase the momentum of light at the surface. So, the apparent wavelength of light may be reduced and as a result field localization beyond the diffraction limit of light can be possible. So, the optical mode can be confined to the sub-wavelength scale, and the size of the optical mode can be minimized. For example, light can be confined to a size 100 times smaller than its wavelength [3, 4, 6-8]. This surface

localization makes plasmonics waveguides an intriguing alternative to conventional dielectric waveguides.

Plasmonics waveguides, based on insulator-metal-insulator (IMI) waveguides, have been studied extensively as well [9, 10]. However, (MDM) waveguides have higher confinement factors and closer spacing to adjacent waveguides [11, 12] and have been proposed for a lot of applications such as Optical resonators, waveguide bends and splitters based on MDM sub-wavelength plasmonics waveguides [13-15].

The MDM waveguides studied previously have nonasymmetric structure, meaning that the metals at the top and bottom of the dielectric layer are the same. Also, asymmetric MDMs have not been investigated, and to the best of our knowledge, a few researchers have investigated the non-asymmetric optical phenomena in these asymmetric waveguides. Moreover, little attention has so far been paid to the SOLITON in plasmonics waveguides, and this issue on MDM plasmonics waveguides is yet to be studied extensively. Among the nonasymmetric processes, SOLITON is frequently studied because of its interesting applications and simple theoretical principle [16]. In Silicon, however, SOLITON cannot be directly excited. The reason is that the second-order susceptibility vanishes in this material, as a result of the crystal centro-symmetry. Exploitation of

Silicon Nitride (Si_3N_4) has been proposed to solve this drawback and induces second-order nonasymmetric processes in Silicon compatible structures [17–20]. More recently, Oliveira et al. reported SOLITON in a 20 μm radius Si_3N_4 ring resonator by using the electric-field induced SOLITON process and calculated a conversion efficiency of about 3.68×10^{-3} with a pumping power of 75 mw [19]. In order to further increase the efficiency of SOLITON and reduce the sizes of devices, the LiNbO_3 crystal in plasmonics based nonasymmetric devices are among the most promising candidates to match this expectation, as a result of their ability to allow strong local-enhanced confinement of light beyond the limits imposed by the laws of diffraction in dielectric media [20]. Several kinds of nonasymmetric plasmonics structures have been proposed. For instance, efficient SOLITON has been presented in plasmonics slot waveguides (PSW) [21], long-range plasmonics waveguides [22], hybrid plasmonics waveguides (HPW) [23], metal surfaces with nanoscale roughness [24], individual metallic nano-aperture [25], plasmonics particle chains [26], and plasmonics core-shell nanowires [27]. From our knowledge, the most used nonasymmetric material in these structures to realize SOLITON is Lithium Niobite [16]. However, in spite of the generally used continuous wave (CW) pump power of the FF to about 1 W, the peak powers of the generated SHF are usually limited to 10^{-5} W [17]. Even if it can be increased to 10^{-2} W in HPW, the corresponding waveguide length to realize this efficiency is 1 mm [18], which is probably too long and not suitable for application in future integrated nanophotonic circuits. The rather small reported efficiencies are due to the relatively small nonasymmetric susceptibility in crystal, the moderately large nonasymmetric coupling coefficients between different frequencies, and the absorption loss of the plasmonics modes. In this paper, for the first time, SOLITON, one of the important nonasymmetric effects, was investigated in asymmetric plasmonics waveguides. For this purpose, different metals, Gold-and-Silver, were used for MDM plasmonics waveguide. It was found that the asymmetric structure (Gold-LiNbO₃-Silver) has higher SOLITON compared to the nonasymmetric structures. Therefore, by using different metals in plasmonics waveguide, the SOLITON have been significantly enhanced compared to conventional structures.

II. THE STRUCTURE OF MDM WAVEGUIDE

Figure 1 shows the MDM plasmonics waveguide structure under consideration. As the figure shows, a crystal slot with thickness a , which is 50 nm, is sandwiched by top and bottom metals. Besides the structure has grating on both sides for more coupling between photons and plasmons. The depth of grating is considered as 30 nm and its duration is optimized to reach the highest second harmonic generation. To optimize the duration of grating, the duration is considered 1500 nm at first and the Soliton enhancement factor is calculated for this duration and for the wavelength

of 458 nm. After that, the duration of grating will be changed for this wavelength and the Soliton will be calculated for every duration. The length of waveguide is 20 μm . So the duration of 1500 nm is equivalent that the number of grooves is 13. So, optimizing the duration is equivalent of optimizing the number of grooves. One of the following metals Gold (Au), Silver (Ag) or Aluminium (Al) is used as metal₁ and metal₂. If metal₁ and metal₂ are the same, the structure is nonasymmetric, and if the top and bottom metals are different, the structure is asymmetric. Therefore, a nonasymmetric MDM waveguide consists of a crystal film surrounded by the same metals, whereas in the asymmetric MDM waveguide, the crystal film is surrounded by different metals. For example, Al- crystal-Al is a nonasymmetric MDM waveguide and Au- Crystal-Ag is asymmetric plasmonics waveguide. As reported, a nonasymmetric plasmonics waveguide can sustain two different modes [5]. A number of different terminologies such as symmetric and anti-symmetric modes, long range surface Plasmon polariton (LRSPP) and short range surface Plasmon polariton (SRSPP), as well as even and odd modes are used in literature to distinguish between the two modes. Concerning asymmetric plasmonics waveguides, two different modes of quasi-symmetric and quasi-anti-symmetric can exist. Similar to the case of nonasymmetric waveguides, this terminology is based on charge distribution across the centre layer of the waveguide. The profile of LRSPP and SRSPP modes in asymmetric structures is different from those in nonasymmetric structures. This asymmetry in modes can cause the crystal to be centro-asymmetry as a result SOLITON to be excited in this structure. In this paper, the terminology of LRSPP and SRSPP have been adopted for both nonasymmetric and asymmetric structures. It has been shown that asymmetric structures have higher SOLITON enhancement factor.

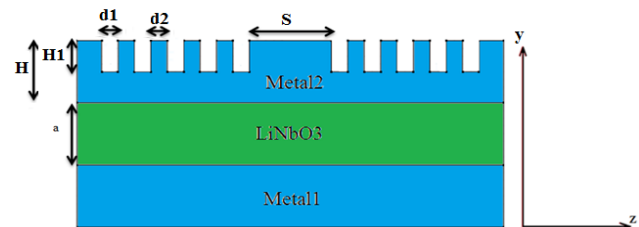


Figure 1. Structure of the MDM waveguide under consideration

In this research, the wavelength of operation of $\lambda=458$ nm was considered. At this wavelength, the permittivity of crystal is $\epsilon_z=5.1772$ and $\epsilon_x=5.6243$, the permittivity of Aluminium is $\epsilon_{Al}=-29 + 7i$, the permittivity of Gold is $\epsilon_{As}=-1.3 + 4.6i$, and the permittivity of Silver is $\epsilon_{Ag}=-6 + 0.66i$.

III. RESULTS AND DISCUSSION

In this section, the simulation results of the different MDM plasmonics waveguides are presented. Different structures including Al-CO-Al, As-CO-As, Ag-CO-Ag, Al-CO-As, Al-CO-Ag, and As-CO-Af were investigated. The simulation results show that asymmetric structures have higher SOLITON enhancement factor. The reason is that the space charge electric field, which couples the two modes, has a asymmetric transverse distribution. Therefore, this asymmetry is said to be favourable in the enhancement of SOLITON. The profile of the electric field amplitude for both nonasymmetric and asymmetric plasmonics waveguides is as shown in Figure 2.

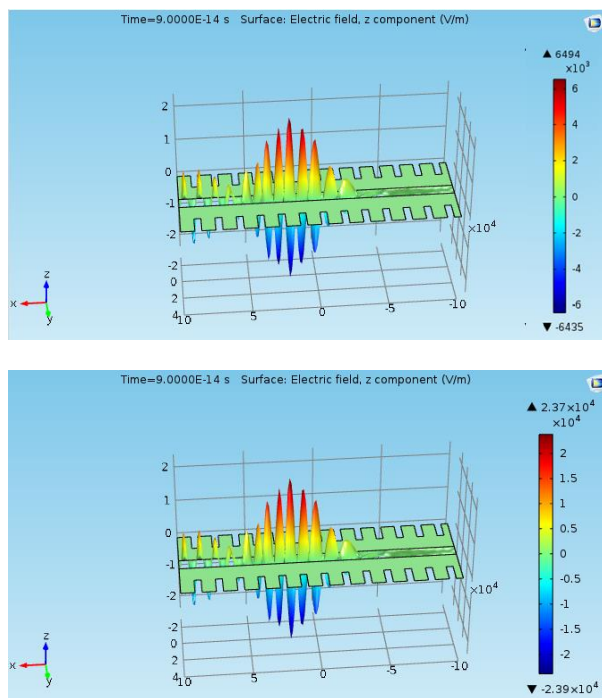


Figure 2. Profile of the electric field amplitude for both non asymmetric (top) and asymmetric plasmonics waveguides (bottom)

It is obvious that the SOLITON is much more significant in the proposed asymmetric structure. In next the number of grooves per unit length is optimized. As mentioned above, the length of waveguide is 20 μm and the number of grooves is changed in this length. Figure 3 shows the electric field amplitude as a function of the number of grooves. One can see that, the electric field magnitude is increased as the number of grooves increased. However, by increasing the number of grooves more than 14, the electric field doesn't change noticeably. So, the number of grooves is considered 14 here.

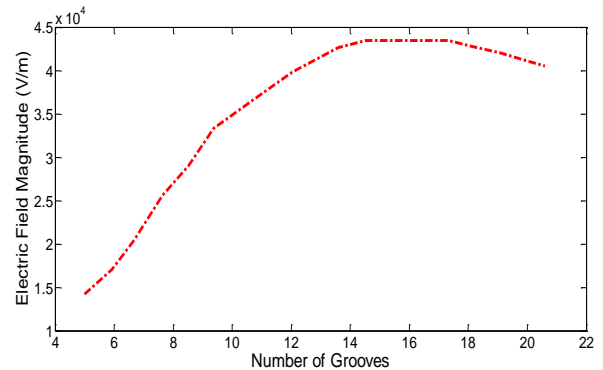


Figure 3. electric field amplitude as a function of the number of grooves

Thus, the SOLITON enhancement factor for different structures as a function of wavelength is shown in Figure 4. We also calculate the SOLITON power for the same volume of nonasymmetric material in a uniform thick slab and for a power density equal to the average power density in the LiNbO₃ core of the input dielectric waveguide. The ratio between these two SOLITON powers defines the enhancement factor of SOLITON.

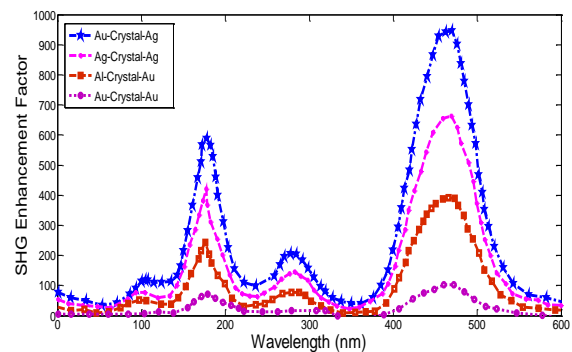


Figure 4. The SOLITON enhancement factor for different structures as a function of wavelength

It was observed in this paper that there is significant enhancement of SOLITON over a broad wavelength range in asymmetric structures. In fact, the Au-Crystal-Ag structure has the most enhanced SOLITON. Figure 5 shows the E_y distributions and frequency spectra of different structures. As shown in the figure, the peak electric field of the proposed structure is dramatically enhanced due to excitation of surface plasmon polaritons (SPPs). Moreover, a second harmonic wave is generated at the center frequency 5.68×10^{14} Hz, and the electric field enhancement consequently led to SOLITON enhancement, as evidenced by the increase in the second harmonic component.

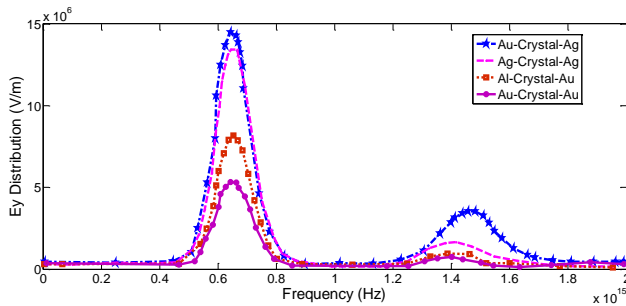


Figure 5. Ey distribution of different structures.

As the crystal thickness changes the surface electric field of second harmonic would be changed as well. Figure 6 shows the surface electric field of second harmonic as a function of crystal thickness. As clear from the figure, there is an optimized point for crystal thickness in which the electric field is maximum. Propagation length of second harmonic field is another important parameter that has to be considered. Figure 7 shows the propagation length of second harmonic as a function of crystal thickness. One can see that by increasing the thickness of the crystal, the propagation length is increased. So, there is an optimized point for crystal thickness in which both the electric field and propagation length of second harmonic is optimized.

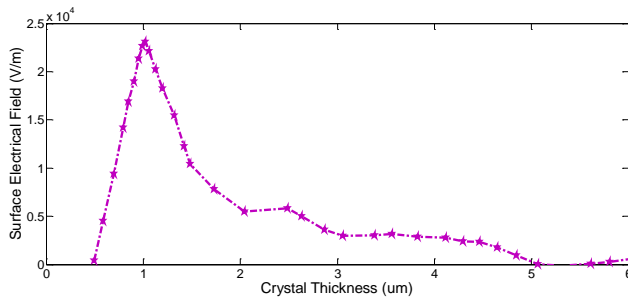


Figure 6 the surface electric field of second harmonic as a function of crystal thickness.

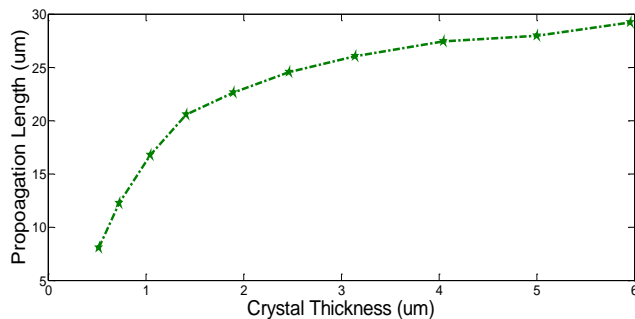


Figure 7 the propagation length of second harmonic as a function of crystal thickness

IV. CONCLUSIONS

In this paper, the SOLITON in nonasymmetric and asymmetric metal-dielectric-metal plasmonics waveguides was investigated. The Lathium Niobite was used as insulator. Different MDM plasmonics waveguides with different metals as cladding layer were studied, and simulation results of the SOLITON in these plasmonics waveguides have been presented. The proposed structure had grating on both sides and the duration per unit length or the number of grooves were optimized to reach the highest second harmonic generation. Two interfering nonasymmetric and asymmetric SPP modes for both nonasymmetric and asymmetric structures were studied. The spatial distribution of the SPP fields for both nonasymmetric and asymmetric structures was considered. It was found that a significant second harmonic wave could be generated in the asymmetric plasmonics waveguides. The crystal thickness of asymmetric MDM waveguide was optimized to achieve the highest second harmonic field. Therefore, asymmetric plasmonics waveguides are a promising structure for future applications of SOLITON.

REFERENCES

- [1]. V. J. Sorger, R. F. Oulton, R.-M. Ma, and X. Zhang, "Toward integrated plasmonics circuits," *MRS Bull.* 37(08), 728–738, (2012).
- [2]. Montasir Qasymeh, "Photorefractive Effect in Plasmonics Waveguides," *IEEE JOURNAL OF QUANTUM ELECTRONICS*, 50(5), 327 – 333, (2014).
- [3]. D. K. Gramotnev and S. I. Bozhevolnyi, "Plasmonics beyond the diffraction limit," *Nature Photon.*, 4, 83–91, (2010).
- [4]. J. A. Schuller, E. S. Barnard, W. Cai, Y. C. Jun, J. S. White, and M. L. Brongersma, "Plasmonics for extreme light concentration and manipulation," *Nature Mater.*, 9, 193–204, (2010).
- [5]. S.A. Maier, "Plasmonics, Fundamentals and Applications" *Springer*, New York, (2007).
- [6]. E. Ozbay, "Plasmonics: Merging photonics and electronics at nanoscale dimensions," *Science*, 311(5758), 189–193, (2006).
- [7]. N. Pleros, E. E. Kriezis, and K. Vysokinos, "Optical interconnects using plasmonics and Si-photonics," *IEEE Journal of Photonics*, 3(2), 296–301, (2011).
- [8]. D. S. LyGagnon, K. C. Balram, J. S. White, P. Wahl, M. L. Brongersma, and D. A. B. Miller, "Routing and photodetection in subwavelength plasmonics slot waveguides," *Journal of Nanophotonics*, 1(1), 9–16, (2012).
- [9]. T. Goto, Y. Katagiri, H. Fukuda, H. Shinojima, Y. Nakano, I. Kobayashi, and Y. Mitsuoka, "Propagation loss measurement for surface plasmon-polariton modes at metal waveguides on semiconductor substrates," *Applied Physics Letters*, 84, 852–854, (2004).
- [10]. R. Charbonneau, N. Lahoud, G. Mattiussi, and P. Berini, "Demonstration of integrated optics elements based on long-ranging surface plasmon polaritons," *Optics Express*, 13, 977–984, (2005).
- [11]. J. A. Dionne, L. A. Sweatlock, and H. A. Atwater, "Plasmon slot waveguides: Towards chip-scale propagation with subwavelength-scale localization," *Physical Review B*, 73, 035407, (2006).

- [12]. R. Zia, M. D. Selker, P. B. Catrysse, and M. L. Brongersma, "Geometries and materials for subwavelength surface plasmon modes," *Journal of the Optical Society of America A*, 21, 2442-2446, (2004).
- [13]. H. T. Miyazaki and Y. Kurokawa, "Squeezing visible light waves into a 3-nm-thick and 55-nm-long plasmon cavity," *Physical Review Letters*, 96, 097401, (2006).
- [14]. Y. Kurokawa and H. T. Miyazaki, "Metal-dielectric-metal plasmon nanocavities: Analysis of optical properties," *Physical Review B*, 75, 035411, (2007).
- [15]. G. Veronis and S. Fan, "Bends and splitters in metal-dielectric-metal subwavelength plasmonics waveguides," *Applied Physics Letters*, 87, 131102, (2005).
- [16]. R. W. Boyd, *Nonasymmetric Optics* (Academic, 2008).
- [17]. M. Cazzanelli, F. Bianco, E. Borga, G. Pucker, M. Ghulinyan, E. Degoli, E. Luppi, V. Vénard, S. Ossicini, D. Modotto, S. Wabnitz, R. Pierobon, and L. Pavesi, "Soliton silicon waveguides strained by silicon nitride," *Nat. Mater.* 11(2), 148-154 (2011).
- [18]. J. S. Levy, M. A. Foster, A. L. Gaeta, and M. Lipson, "Harmonic generation in silicon nitride ring resonators," *Opt. Express* 19(12), 11415-11421 (2011).
- [19]. R. E. P. de Oliveira, M. Lipson, and C. J. S. de Matos, "Electrically controlled silicon nitride ring resonator for quasi-phase matched second-harmonic generation," in *CLEO: Science and Innovations* (Optical Society of America, 2012).
- [20]. T. Y. Ning, H. Pietarinen, O. Hyvärinen, R. Kumar, T. Kaplas, M. Kauranen, and G. Genty, "Efficient secondharmonic generation in silicon nitride resonant waveguide gratings," *Opt. Lett.* 37(20), 4269-4271 (2012).
- [21]. M. L. Brongersma and P. G. Kik, *Surface Plasmon Nanophotonics* (Springer, 2007).
- [22]. M. I. Stockman, "Nanoplasmonics: past, present, and glimpse into future," *Opt. Express* 19(22), 22029-22106 (2011).
- [23]. W. S. Cai, A. P. Vasudev, and M. L. Brongersma, "Electrically controlled nonasymmetric generation of light with plasmonics," *Science* 333(6050), 1720-1723 (2011).
- [24]. A. R. Davoyan, I. V. Shadrivov, and Y. S. Kivshar, "Quadratic phase matching in nonasymmetric plasmonics nanoscale waveguides," *Opt. Express* 17(22), 20063-20068 (2009).
- [25]. S. B. Hasan, C. Rockstuhl, T. Pertsch, and F. Lederer, "Second-order nonasymmetric frequency conversion processes in plasmonics slot waveguides," *J. Opt. Soc. Am. B* 29(7), 1606-1611 (2012).
- [26]. A. Ashkin, G. D. Boyd, J. M. Dziedzic, R. G. Smith, A. A. Ballman, J. J. Levinstein, and K. Nassau, "Optically-induced refractive index inhomogeneities in LiNbO₃ and LiTaO₃," *Applied Physics Letters*, 9(1), 72-74, (1966).
- [27]. A. Yariv, "Phase conjugate optics and real-time holography," *IEEE Journal of Quantum Electronics*, 14(9), 650-660, (1978).